Bioorganic & Medicinal Chemistry Letters 19 (2009) 912–916

Contents lists available at ScienceDirect

Bioorganic & Medicinal Chemistry Letters

journal homepage: www.elsevier.com/locate/bmcl

2-Aminoimidazoles inhibitors of TGF-β receptor 1

Dominique Bonafoux [a,*], Claudio Chuaqui [b], P. Ann Boriack-Sjodin [b], Chris Fitch [b], Gretchen Hankins [b], Serene Josiah [b], Cheryl Black [b], Gregg Hetu [b], Leona Ling [b], Wen-Cherng Lee [b,*]

[a] Abbot Laboratories, 381 Plantation Street, Worcester, MA 01605-2323, USA
[b] BiogenIdec, 14 Cambridge Street, Cambridge, MA 02142, USA

ARTICLE INFO

Article history:
Received 3 October 2008
Revised 25 November 2008
Accepted 26 November 2008
Available online 11 December 2008

Keywords:
2-Amidoimidazoles
TGF-βR1
X-ray structure
PK

ABSTRACT

The 4-(5-fluoro-6-methyl-pyridin-2-yl)-5-quinoxalin-6-yl-1H-imidazol-2-ylamine **3** is a potent and selective inhibitor of TGF-βR1. Substitution of the amino group of **3** typically led to a slight decrease in the affinity for the receptor and in TGF-β-inducted PAI-luciferase reporter activity. However, 2-acetamidoimidazoles were identified as attractive candidates for further optimization as a result of their significant activity combined to their superior pharmacokinetic profile.

Transforming growth factor-beta (TGF-β) is an ubiquitous cytokine that affects various biological processes such as regulation of cell proliferation, immune responses, growth, differentiation, angiogenesis, and apoptosis of various cell types. The TGF-β ligand initiates signaling through binding to the type 2 receptor (TGF-βR2), a serine/threonine kinase, expressed on the cell surface. Upon ligand binding, a hetero-tetrameric complex consisting of two type 2 receptors and two type 1 receptors (TGF-βR1 or activin-like kinase receptor-5 (ALK-5)) is formed. In the receptor complex, the ligand-bound type 2 receptor phosphorylates the TGF-βR1 in the GS region (glycine/serine rich domain), which, in turn, allows the type I receptor to phosphorylate the transcriptional regulators, Smad2 and Smad3.[1] Phosphorylated Smad2 or Smad3 then complex with Smad4. The resulting hetero-Smad complex finally translocates to the nucleus to trigger the regulation of various TGF-β-responsive genes.[2] TGF-βR1 represents a key target for the pharmaceutical industry. In particular, small molecules inhibitors of TGF-βR1 offer an attractive way to regulate the TGF-β pathway and can therefore find applications in the treatment of various diseases, in particular, cancer.[3]

Our on-going interest in imidazole-based TGF-βR1 inhibitors[4] and recent reports about 2-aminothiazoles showing ALK-5 inhibition,[5] led us to synthesize novel 2-aminoimidazoles[6] and evaluate them in vitro for their ability to (i) bind to human TGF-βR1[7] and (ii) inhibit the TGF-β-inducted PAI-luciferase reporter activity in transfected HepG2 cells.[8]

The 4-(5-fluoro-6-methyl-pyridin-2-yl)-5-quinoxalin-6-yl-1H-imidazol-2-ylamine **3** was synthesized via bromination of the 1-(5-fluoro-6-methyl-pyridin-2-yl)-2-quinoxalin-6-yl-ethanone **1**[4] followed by condensation of the resulting bromoketone **2** with *N*-acetylguanidine[9] before acidic deprotection of the amino group (Scheme 1). According to previous reports on related compounds,[5,10,11] both the 2-pyridyl and the quinoxalinyl-substituents are involved in key interactions with human ALK-5. The nitrogen of the 2-pyridyl group is engaged in a water mediated hydrogen bond network with the side chains of Tyr-249 and Glu-245 as well as the backbone of Asp-351, while the quinoxalinyl substituent directly binds to the backbone of His-283 in the hinge region. Aminoimidazole **3**, bearing both the 2-pyridinyl- and the quinoxalinyl-substituents, was therefore predicted to be a potent inhibitor. This expectation was confirmed with a subnanomolar affinity for TGF-βR1 (K_i = 0.7 nM) and a very significant inhibition of PAI reporter activity (IC_{50} = 33.5 nM). Compound **3** was also evaluated on p38,[12] because of its structural similarity to known p38 inhibitors,[13] and showed not activity (IC_{50} = 12.5 μM). Interestingly, acetamidoimidazole precursor **2** also exhibited noticeable inhibition of TGF-βR1 with a K_i of 7.1 nM, indicating that some degree of substitution of the 2-amino group in **3** can be tolerated without complete loss of potency. In the light of this result, we assessed 2-acetylated aminoimidazoles **2** and **6–11**, as well as substituted 2-aminoimidazoles **16–20** for their ability to inhibit TGF-βR1.

2-Acetamidoimidazoles **6** and **7**, bearing a triazolo[1,5-*a*]pyridinyl substituent in the hinge region, were synthesized following the conditions highlighted in Scheme 1, from the 1-(6-methyl-pyridin-2-yl)- (**4**) and the 1-(5-fluoro-6-methyl-pyridin-2-yl)-2-

* Corresponding authors.
E-mail addresses: dominique.bonafoux@abbott.com (D. Bonafoux), wen-cherng.lee@biogenidec.com (W.-C. Lee).

0960-894X/$ - see front matter © 2008 Elsevier Ltd. All rights reserved.
doi:10.1016/j.bmcl.2008.11.119

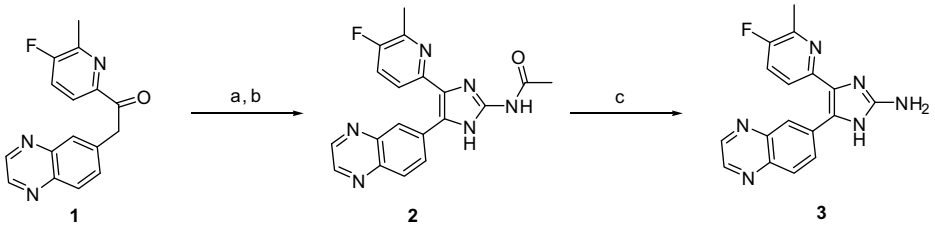

Scheme 1. Reagents and conditions: (a) Br_2, dioxane, rt, quantitative; (b) *N*-acetylguanidine, CH_3CN, 1 h, 40%; (c) H_2SO_4, MeOH, reflux 4 h, 60%.

[1,2,4]triazolo-[1,5-*a*]pyridin-6-yl-ethanones (**5**).[4] The 2-methylpropionyl- (**8**), propionyl- (**9**), methoxyacetyl- (**10**), and methoxypropionyl- (**11**) analogs, were also prepared according to Scheme 1, using acylated guanidines that were obtained via addition of guanidine to the suitable ethylesters[14] (Scheme 2).

The 2-piperidinyl- (**16**), the 2-morpholino- (**17**) and 2-piperazinyl derivatives (**18–20**) were synthesized, with yields ranging from 12% to 40%, through the condensation of the 1-(5-fluoro-6-methyl-pyridin-2-yl)-2-[1,2,4]triazolo[1,5-*a*]pyridin-6-yl-ethane-1,2-dione (**15**) with substituted guanidines, followed by Pd/C-catalyzed dehydration (Scheme 3).[15]

The acetamidoimidazoles **2**, **6** and **7** displayed comparable affinities for TGF-βR1 with K_i values ranging from 2.07 nM to 7.1 nM and comparable levels of inhibition of TGF-β-inducted PAI-luciferase reporter activity with IC_{50}s between 110 and 180 nM and were selective versus p38. These results demonstrated that the quinoxaline and the triazolo[1,5-*a*]pyridine series offer similar overall profiles (Table 1). As a result, both series will be treated as fully comparable during this work.

The replacement of the acetyl group in **2** with flexible linear groups, such as, propionyl- (**9**), methoxyacetyl- (**10**) and methoxypropionyl- (**11**) did not affect the affinity for TGF-βR1 at all, whereas the introduction of the bulkier methylpropionyl-group (**8**) led to a complete loss of potency (Table 2).

Acylated imidazoles **2**, **6**, **7** and **9–11** showed comparable levels of inhibition of TGF-β-inducted PAI-luciferase reporter activity as well as selectivity towards p38.

Tightening the 2-amino group of **3** to form a six membered ring (**16–20**), much like the corresponding acylation, led to a slight decrease in affinity for the receptor with K_i values typically ranging from 3 nM to 16.4 nM (Table 3). The absence of a polar substituent at position 4 of the six membered ring was found to be rather unfavorable, since the 2-piperidinylimidazole **16** suffered an average 3.5-fold decrease in affinity for the receptor compared to 2-morpholino- (**17**), 2-(*N*-methylpiperazinyl)- (**18**), 2-(*N*-acetylpiperazinyl)- (**19**) and 2-(*N*-methanesulfonyl-piperazinyl)-imidazole (**20**). 2-Aminoimidazoles **17–20** showed a cellular activity overall comparable to the acylated analogs.

In order to confirm the binding mode for the acetylated imidazoles, the structure of **2** complexed to hu-TGF-βR1 was solved with crystallographic methods using procedures previously described.[11] The 3.2 Å structure has an R_{factor} and R_{free} of 0.231 and 0.279, respectively.[16] The data confirmed that the quinoxaline ring binds to the hinge region and accepts a hydrogen bond from the NH of His-283 and that the fluoro-methylpyridine ring binds in the hydrophobic pocket. In addition, the NH of the aminoacetyl group in **2** donates a hydrogen bond to the side chain of Asp-351. It is worth noting that, even though Asp 351 has previously been shown to accept a hydrogen bond from pyrazole based inhibitors,[11] in the structure of **2** in TGF-βR1 the Asp 351 side chain has rotated ~45 deg about chi1 and shifted the position of the acid carbonyl 1.8 Å in order to accommodate the substitution off the imidazole ring (Fig. 1).

Using the co-crystal structure of **2** complexed to TGF-βR1, we carried out ligand receptor docking[17] in order to help rationalize the SAR presented in Table 2. In particular, we sought to understand why the methylpropionyl substituent in **8** was not tolerated whereas more flexible linear groups, such as in **9–11**, did not lead to a loss of potency. The crystallographically observed binding mode of **2** was recapitulated via molecular docking to within 0.1 Å, thus preserving the hydrogen-bonding patterns observed in the X-ray co-crystal structure. The top scoring poses generated from docking of the linearly substituted analogs **9–11** were predicted to bind in the same mode as was observed for **2**. For these ligands, the imidazole core, quinoxaline substituent at the hinge, and the fluoro-methylpyridine ring in the hydrophobic pocket, of the docked poses were nearly overlapped with the corresponding groups in the X-ray structure. In other words, the acyl substituents did not disrupt any of the hydrogen bonding and hydrophobic interactions observed in the X-ray co-crystal. For these ligands, the linear acyl substituents were predicted to extend into the region next to the p-loop of the kinase. In contrast, docking was not able to generate a pose for **8** that preserved the interactions observed in the X-ray structure. The top scoring poses required at least a 0.5 Å shift of the ligand, presumably to accommodate the bulkier methylpropionyl substituent. Although the predicted shifted binding mode of **8** is generally similar to that of **2**, each of the hydrogen bonds to the receptor is weakened substantially. In addition, the planarity of the amide bond in **8** is compromised in every docked pose, introducing ligand strain not present in the docked poses of compounds **2**, **9–11**. These factors serve as an acceptable rationale for the observed lack of activity of **8** (Fig. 2).

In order to establish the impact of the substitution pattern of 2-aminoimidazoles on their pharmacokinetic profiles, acylated

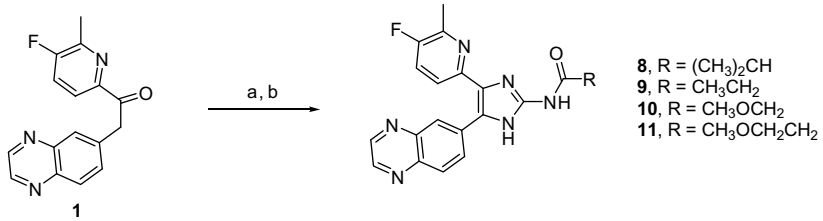

Scheme 2. Reagents and conditions: (a) Br_2, dioxane, rt, quantitative; (b) *N*-acylguanidine, CH_3CN, 1 h, 13–36%.

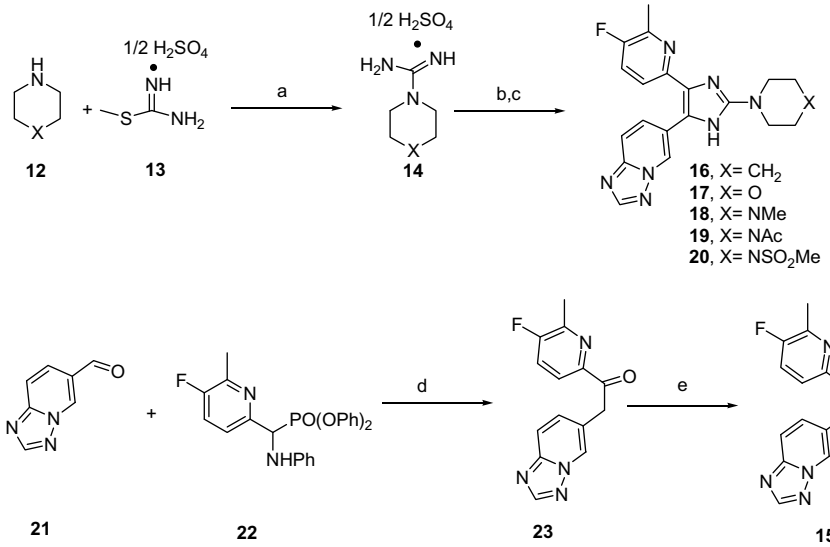

Scheme 3. Reagents and conditions: (a) EtOH, reflux, 70–95%; (b) **15**, Na_2CO_3, MeOH, rt; (c) Pd/C, H_2 (20 psi), MeOH, rt, 12–40%; (d) THF/*i*-PrOH (4/1), rt, 78%; (e) DMSO, 120 °C, 74%.

Table 1
Inhibitory profile for acetamidoimiadazoles **2**, **6** and **7**

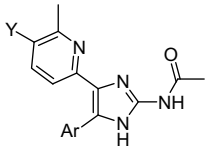

	Ar	Y	TGF-βR1 K_i[a] (nM)	PAI EC_{50}[a] (nM)	p38 EC_{50}[a] (μM)
2	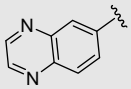	F	7.1	180	14.8
6	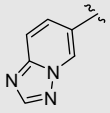	H	2.95	165	57.8
7	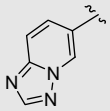	F	2.07	111	28.1

[a] Averaged values ($n = 2$).

Table 2
Inhibitory profile for various acylated imidoimiadazoles **8–11**

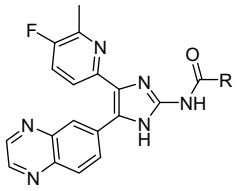

	R	TGF-βR1 K_i[a] (nM)	PAI EC_{50}[a] (nM)	p38 EC_{50}[a] (μM)
2	CH_3	7.1	180	14.8
8	$(CH_3)_2CH$	>28,000	nd	nd
9	CH_3CH_2	8.8	156	13.53
10	CH_3OCH_2	7.2	61	15.0
11	$CH_3OCH_2CH_2$	19	148	14.83

[a] Averaged values ($n = 2$).

Table 3
Inhibitory profile for various 2-aminoimidoimiadazoles **15–19**

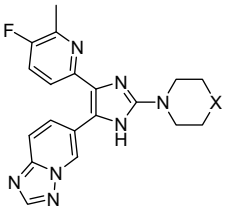

	X	TGF-βR1 K_i[a] (nM)	PAI EC_{50}[a] (nM)	p38 EC_{50}[a] (μM)
16	CH_2	53.2	nd	nd
17	O	15	513	46.3
18	NMe	16.4	344	10.9
19	NAc	15.2	1220	14.2
20	NSO_2Me	3	414	41.2

[a] Averaged values ($n = 2$).

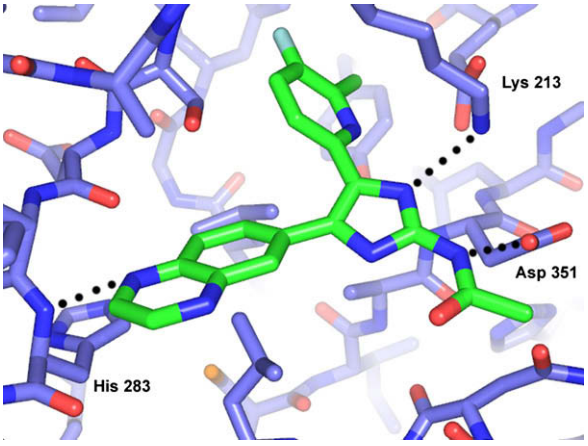

Figure 1. Interactions of **2** in the TGF-βR1 active site. Hydrogen bonds are shown as dotted lines.

imidazoles **2**, **6** and **11** as well as 2-aminoimidazoles **3** and **17** were evaluated in rat PK. The data is summarized in Table 4 and unambiguously shows that the nature of the substituent on the 2-amino

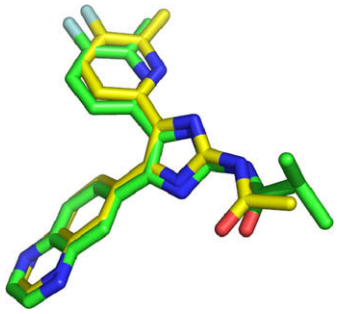

Figure 2. Docked structures of **2** (yellow) and **8** (green) overlaid.

Table 4
Selected pharmacokinetic parameters for the oral administration of acetamio- and aminoimidazoles to fasted male Sprague–Dawley rats

Compound	$T_{1/2}$[a] (h)	F[b] (%)
2[c]	7.8	66
6[c]	7.1	100
11[c]	13.2	41
3[d]	0.6	28
17[c]	0.4	25
25[c]	7.4	87

[a] Values are means of 4 iv experiments.
[b] Values are means of 8 experiments (4 iv, 4 po).
[c] Vehicle, 20% captisol.
[d] Vehicle, NMP/H_2O (1/1).

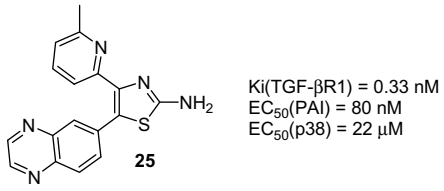

Figure 3. Structure of the 2-aminothiazole **24** and its in vitro data.

group dramatically impacts the PK profile, since the acylated imidazoles **2**, **6** and **11** displayed a superior profile compared to 2-aminoimidazoles **3** and **17**, with higher bioavailabilities 66%, 100% and 41%, respectively, versus 28% and 25% and longer half-lives of 7.8 h, 7.1 h and 13.2 h versus 0.6 h and 0.4 h.

Furthermore, a comparison between the unsubstituted 2-aminoimidazole **3** and the closely related unsubstituted 2-aminothiazole derivative **25** (Fig. 3) indicated that switching from a imidazole to a thiazole core was also a favorable modification. This imidazole/thiazole switch is thus a structural change that could be used to fine tune the PK profile of such inhibitors in further studies.

In conclusion, we have confirmed that 2-aminoimidazoles and 2-acetamidoimidazoles are potent and selective inhibitors of TGF-βR1. We found that tightening the nitrogen at position 2 of the imidazole within a six membered ring or acylating it with flexible linear groups led to a slight decrease in potency (up to 10-fold on TGF-βR1 binding affinity and about 5-fold on the inhibition of TGF-β-inducted PAI-luciferase reporter activity) compared to fully unsubstituted analog **3**. This slight decrease in potency is however compensated for, in the case of 2-acetamidoimidazoles **2**, **6** and **11** with a superior pharmacokinetic profile. These results indicate that acylated 2-aminoimidazoles TGF-βR1-inhibitors, in particular 2-acetamidoimidazole **6**, provide attractive, orally bioavailable candidates for further in vivo studies.

References and notes

1. (a) Huse, M.; Muir, T. W.; Xu, L.; Chen, Y.; Kuriyan, J.; Massague, J. *Mol. Cell* **2001**, *8*, 671; (b) Miyazawa, K.; Shinozaki, M.; Hara, T.; Furuya, T.; Miyazono, K. *Genes Cells* **2002**, *7*, 1191.
2. Massagué, J. *Ann. Rev. Biochem.* **1998**, *67*, 773.
3. Lahn, M.; Klocker, S.; Berry, B. S. *Expert. Opin. Invest. Drugs* **2005**, *14*, 629.
4. Lee, W. -C.; Sun, L.; Shan, F.; Chuaqui, C.; Zheng, Z.; Petter, R. C. WO 2003087304; Lee, W. -C.; Chuaqui, C.; Sun, L.; Hoemann, M.; Niu, D.; Yan, D; Petter, R. C.; Feng, H. WO 2007076086; Lee, W. -C.; Chuaqui, C.; Sun, L.; Hoemann, M.; Niu, D.; Yan, D.; Bonafoux, D.; Cornebise, M. WO 2007076127.
5. (a) Gellibert, F.; Woolven, J.; Fouchet, M.-H.; Mathews, N.; Goodland, H.; Lovegrove, V.; Laroze, A.; Nguyen, V.-L.; Sautet, S.; Wamg, R.; Jason, C.; Smith, W.; Krysa, G.; Boullay, V.; de Gouville, A.-C.; Huet, S.; Hartley, D. *J. Med. Chem.* **2004**, *47*, 4494; (b) Kim, D.-K.; Choi, J. H.; An, Y. J.; Lee, H. S. *Bioorg. Med. Chem. Lett.* **2008**, *18*, 2122.
6. While this manuscript was in preparation a series of 2-aminoimidazole TGF-β inhibitors was reported Kim, D.-K.; Jang, Y.; Lee, H. S.; Park, H.-J.; Yoo, J. *J. Med. Chem.* **2007**, *50*, 3143.
7. The binding reactions were carried out in 100 μl of buffer A (0.1% Tween-20, 30 mM HEPES hemisodium salt, pH 7.5, 100 mM KCl, 20 mM NaCl, 1 mM $MgCl_2$, 0.1% bovine serum albumin, 1% dimethyl sulfoxide) in a ThermoLabsystems black 96-well microfluor 2 plate #7205 (www.thermo.com), using 25 nM F-KL (a fluorescence-labeled ALK-5 inhibitor) and 5 nM ALK-5. The inhibitor was added at various concentrations and incubated at room temperature for 60 min, then read on a fluorescent plate reader (LJL Analyst, Molecular Devices) with 10 nm bandpass filters set at 490 and 530 nm. Measurements were reported in milli-polarization (mP). K_d measurements were performed in triplicate and are representative of four independent measurements. Data analysis was performed using Prism (Graphpad Software) with quadratic and hyperbolic fits. K_d values and fits were comparable by both methods and data from hyperbolic fit is shown. IC_{50} measurements were performed as 10-point curves with 3× dilution series where each point was measured in duplicate. Each IC_{50} value is representative of three independent measurements. K_i values were obtained by Cheng–Prusoff conversion from the measured K_d for F-KL and the IC_{50} value obtained for a given inhibitor. Data analysis was performed by Prism (Graphpad software) with 4-parameter fit. All binding reactions were performed in a 96-well plate format with control wells to define non-specific binding containing 1 mM ATP. The reference compound used in this assay is SM16.[12]
8. HepG2 cells were stably transfected with the PAI-luciferase reporter grown in DMEM medium containing 10% FBS, penicillin (100 U/ml), streptomycin (100 μg/ml), L-glutamine (2 mM), sodium pyruvate (1 mM), and non essential amino acids (1×). The transfected cells were then plated at a concentration of 2.5×10^4 cells/well in 96-well plates and starved for 3–6 h in media with 0.5% FBS at 37 °C in a 5% CO_2 incubator. The cells were then stimulated with ligand either 2.5 ng/ml TGFβ in the starvation media containing 1% DMSO and the presence or absence of test compounds of formula (I) and incubated as described above for 24 h. The media was washed out in the following day and the luciferase reporter activity was detected using the LucLite Luciferase Reporter Gene Assay kit (Packard, cat. No. 6016911) as recommended. The plates were read on a Wallac Microbeta plate reader. The reference compound used in this assay is SM16.[12]
9. Little, T. L.; Webber, S. E. *J. Org. Chem.* **1994**, *59*, 7299.
10. Sawyer, J. S.; Anderson, B. D.; Beight, D. W.; Campbell, R. M.; Jones, M. L.; Herron, D. K.; Lampe, J. W.; McCowan, J. R.; McMillen, W. T.; Mort, N.; Parsons, S.; Smith, E. C. R.; Vieth, M.; Weir, L. C.; Yan, L.; Zhang, F.; Yingling, J. M. *J. Med. Chem.* **2003**, *46*, 3953.
11. Singh, J.; Chuaqui, C. E.; Boriack-Sjodin, A. P.; Lee, W.-C.; Pontz, T.; Corbley, M. J.; Cheung, H.-K.; Arduini, R. M.; Mead, J. N.; Newman, M. N.; Papadatos, J. L.; Bowes, S.; Josiah, S.; Ling, L. E. *Bioorg. Med. Chem. Lett.* **2003**, *13*, 4355.
12. For p38 assay conditions see: Fu, K.; Corbley, M. J.; Friedman, J. E.; Shan, F.; Papadatos, J. L.; Costa, D.; Lutterodt, F.; Sweigard, H.; Bowes, S.; Choi, M.; Boriack-Sjodin, A.; Arduini, R. M.; Sun, D.; Newman, M. N.; Zhang, X.; Mead, J. N.; Chuaqui, C. E.; Cheung, H.-K.; Zhang, X.; Cornebise, M.; Carer, M.; Josiah, S.; Singh, J.; Lee, W.-C.; Gill, A.; Ling, L. E. *Arterioscler. Thromb. Vasc. Biol.* **2008**, *28*, 665.
13. For examples of 2,4,5-trisubstituted imidazoles p38 inhibitors see: (a) Koch, P.; Baeuerlein, C.; Jank, H.; Laufer, S. *J. Med. Chem.* **2008**, *51*, 5630; (b) Kim, D.-K.; Lim, J.-H.; Lee, Jung A.; Dewang, P. M. *Bioorg. Med. Chem. Lett.* **2008**, *18*, 4006; (c) McClure, K. F.; Letavic, M. A.; Kalgutkar, A. S.; Gabel, C. A.; Audoly, L.; Barberia, J. T.; Braganza, J. F.; Carter, D.; Carty, T. J.; Cortina, S. R.; Dombroski, M. A.; Donahue, K. M.; Elliott, N. C.; Gibbons, C. P.; Jordan, C. K.; Kuperman, A. V.; Labasi, J. M.; LaLiberte, R. E.; McCoy, J. M.; Naiman, B. M.; Nelson, K. L.; Nguyen, H. T.; Peese, K. M.; Sweeney, F. J.; Taylor, T. J.; Trebino, C. E.; Abramov, Y. A.; Laird, E. R.; Volberg, W. A.; Zhou, J.; Bach, J.; Lombardo, F. *Bioorg. Med. Chem. Lett.* **2006**, *16*, 4339; (d) Norris, J. L.; Williams, K. P.; Janzen, W. P.; Hodge, C. N.; Blackwell, L. J.; Popa-Burke, I. G. *Lett. Drug Design Discov.* **2005**, *2*, 516.
14. Viscontini, M.; Bally, J.; Meier, J. *Helv. Chim. Acta* **1952**, *35*, 451.
15. Nishimura, T.; Kitajima, K. *J. Org. Chem.* **1979**, *44*, 818.
16. X-ray coordinates deposited with the RCSB Protein Data Bank: PDB code is 3FAA.
17. Compounds **2**, **8–11** were prepared for docking using Ligprep[18] to generate 3-dimensional ligands with appropriate tautomers and flexible ring conformers. The docking grids were generated with the default settings based on the co-

crystal structure of 2 with TGFβ-R1.Flexible ligand docking was carried out using Glide[19–21] with Extra Precision (XP) scoring. For each ligand, five poses were retained for further analysis and comparison with the binding mode of 2. Visual inspection of the docking results was done using Maestro(5).[22]
18. Ligprep version 2.0 Schrödinger, LLC: Portland, OR.
19. Glide version 3.5 Schrödinger, LLC: Portland, OR.
20. Friesner, R. A.; Banks, J. L.; Murphy, R. B.; Halgren, T. A.; Klicic, J. J.; Mainz, D. T.; Repasky, M. P.; Knoll, E. H.; Shelley, M.; Perry, J. K.; Shaw, D. E.; Francis, P.; Shenkin, P. S. *J. Med. Chem.* **2004**, *47*, 1739.
21. Halgren, T. A.; Murphy, R. B.; Friesner, R. A.; Beard, H. S.; Frye, L. L.; Pollard, W. T.; Banks, J. L. *J. Med. Chem.* **2004**, *47*, 1750.
22. Maestro version 7.0 Schrödinger, LLC: Portland, OR.